

# **Gd plasma source modeling at 6.7 nm for future lithography**

Bowen Li<sup>1</sup>, Padraig Dunne<sup>1</sup>, Takeshi Higashiguchi<sup>2,3</sup>, Takamitsu Otsuka<sup>2</sup>,  
Noboru Yugami<sup>2,3</sup>, Weihua Jiang<sup>4</sup>, Akira Endo<sup>5</sup>, and Gerry O'Sullivan<sup>1</sup>

<sup>1</sup>*School of Physics, University College Dublin, Belfield, Dublin 4, Ireland*

<sup>2</sup>*Department of Advanced Interdisciplinary Sciences, Center for Optical Research & Education (CORE), and Optical Technology Innovation Center (OpTIC), Utsunomiya University, Yoto 7-1-2, Utsunomiya, Tochigi 321-8585 Japan*

<sup>3</sup>*Japan Science and Technology Agency, CREST, 4-1-8 Honcho, Kanagawa, Saitama 332-0012 Japan*

<sup>4</sup>*Department of Electrical Engineering, Nagaoka University of Technology, Kami-tomiokamachi 1603-1, Nagaoka, Niigata 940-2188 Japan*

<sup>5</sup>*Research Institute of Science and Engineering, Waseda University, 3-4-1, Okubo, Shinjuku-ku, Tokyo, Japan 169-0072*

## **Abstract**

Plasmas containing gadolinium have been proposed as sources for next generation lithography at 6.x nm. To determine the optimum plasma conditions, atomic structure calculations have been performed for  $\text{Gd}^{11+}$  to  $\text{Gd}^{27+}$  ions which showed that  $n=4 - n=4$  resonance transitions overlap in the 6.5 – 7.0 nm region. Plasma modeling calculations, assuming collisional-radiative equilibrium, predict that the optimum temperature for an optically thin plasma is close to 110 eV and that maximum intensity occurs at 6.76 nm under these conditions. The close agreement observed between simulated and experimental spectra from laser and discharge produced plasmas indicates the validity of our approach.

The search for the optimum radiation source at 13.5 nm for extreme ultraviolet lithography (EUVL) has been the subject of intense research activity in recent years [1,2]. These studies have shown that plasmas containing tin, where transitions of the type  $4p^6 4d^n - 4p^5 4d^{n+1} + 4d^{n-1} 4f$  overlap in ion stages from  $\text{Sn}^{9+}$  -  $\text{Sn}^{13+}$  to form an unresolved transition array (UTA) centered near 13.5 nm are the strongest emitters at this wavelength. To keep pace with Moore's law, research on shorter wavelength EUV sources has already begun [3-8]. Switching to a shorter wavelength of around 6.5–6.7 nm while maintaining or increasing throughput in the lithography system would improve resolution by a further factor of two [3]. The possibility of a new source wavelength of 6.x nm has emerged due to progress in the fabrication of  $\text{B}_4\text{C}$  ( $\text{La}/\text{B}_4\text{C}$  or  $\text{Mo}/\text{B}_4\text{C}$ ) multilayers with a reflectivity of  $\sim 40\%$  in a 0.06 nm bandwidth near 6.7 nm [9] whose maximum theoretical reflectivity is close to 70% [10].

The precise value of x will be determined by the source emission and reflectivity combination that provides optimum efficiency and in-band EUV yield and its determination is a priority. Following the earliest studies on extreme ultraviolet (EUV) emission from laser produced plasmas of elements with  $62 \leq Z \leq 74$ , it is evident that both Gd and Tb ions have  $4p^6 4d^n - 4p^5 4d^{n+1} + 4d^{n-1} 4f$  transitions near this wavelength and emit an intense unresolved transition array (UTA) [11]. Recently, the suitability of Nd:yttrium-aluminum-garnet (Nd:YAG) laser-produced plasma (LPP) EUV

sources based on Gd and Tb has been demonstrated for high power operation [3,7]. In order to achieve higher conversion efficiency (CE) from laser energy to EUV emission energy and spectral purity, the effects of optical thickness were evaluated by changing the laser wavelengths to change the plasma density and opacity [8]. The spectra of vacuum spark and laser plasma emission of Gd and Tb were first analyzed by Churilov and co-workers [4]. Theoretical spectra were subsequently calculated by Kilbane and O'Sullivan using the Flexible Atomic Code (FAC) for Gd and Tb plasmas [5] and Sasaki *et al.* using the HULLAC code for Tb plasmas [6]. It should be noted that there are discrepancies between these two theoretical simulations [5,6].

In this letter, we report the EUV spectra of Gd calculated with the Hartree-Fock with configuration interaction (HF-CI) method, using the Cowan suite of codes [12], as well as the comparison of the calculated synthetic spectra with laser produced plasmas (LPP) and discharged produced plasmas (DPP). We also show that the optimum plasma temperature is close to 110 eV for an optically thin plasma. Because of the lower critical density, CO<sub>2</sub> LPP are optically thinner than those produced by a Nd:YAG laser.

It has been shown that configuration interaction (CI) plays an important role in the simulation of Gd spectra [4,5], so the choice of electronic configurations to be used is critical. The configurations chosen in the present case are given in

Table I.

**Table I. Electronic configuration models used in the calculations**

Gd XII – Gd XV	Gd XIX	Gd XX – Gd XXVIII
$4d^{10}5s^q4f^n$	$4p^64d^{10}$	$4p^64d^n$
$4d^95s^q4f^{n+1}$	$4p^64d^9nl$	$4p^64d^{n-1}nl$
$4d^{10}5s^q4f^{n-1}(5d,5g)$	$4p^54d^{10}5s$	$4p^54d^{n+1}$
$4d^95s^q4f^n(5p,5f)$		$4p^54d^n5s$
$(0 \leq q \leq 2, 3 \leq n \leq 4)$	$(n \leq 6, l \leq 3)$	$(n \leq 6, l \leq 3)$

The positions and oscillator strengths (gf-values) of the resonance  $4d^{10}4f^n - 4d^94f^{n+1}$ ,  $4d^{10}4f^n - 4d^{10}4f^{n-1}5d$ , and  $4d^{10}4f^n - 4d^{10}4f^{n-1}5g$  transitions for the ions with an outermost 4f subshell ( $Gd^{11+} - Gd^{17+}$ ) and  $4p^64d^n - 4p^54d^{n+1} + 4d^{n-1}4f$ ,  $4p^64d^n - 4p^64d^{n-1}5p$ , and  $4p^64d^n - 4p^64d^{n-1}5f$  transitions for ions with an outermost 4d subshell ( $Gd^{18+} - Gd^{27+}$ ) were calculated and are shown in Fig. 1. It is obvious from this figure that transitions of the type  $4d^{10}4f^n - 4d^94f^{n+1}$ , not present in Sn, may also contribute to the in-band emission. Thus many ion stages can contribute and strong emission is expected over a wide range of plasma temperatures. Because of the high line density, the transitions were treated within the UTA formalism [13] and the intensity weighted mean positions and widths of the arrays were calculated and the results are presented in Fig. 2. From both Figs. 1 and 2 it can be seen that the mean

position of the  $\Delta n = 0$ ,  $n = 4 - n = 4$  transitions initially moves to shorter wavelength as the degree of ionization increases and when the 4f subshell empties, this mean position reverses direction with increasing ionization. In all reported studies of  $n = 4 - n = 4$  transitions the emission is dominated by Pd-, Ag- and Rh-like lines [4, 14, 16 -18], i.e. the spectra containing fewest lines where the emission is not divided amongst many transitions. So, the optimum plasma condition should maximize the populations of these ion stages.

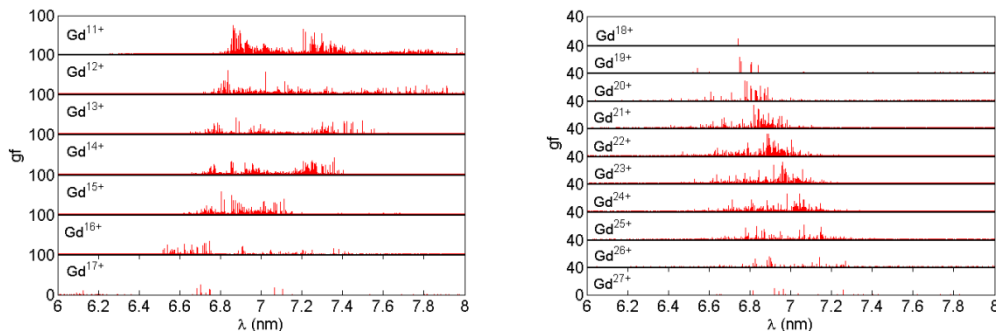


*Fig. 1: Calculated spectra (oscillator strength vs  $\lambda$ ) for Gd ions in the 6-8 nm spectral region.*

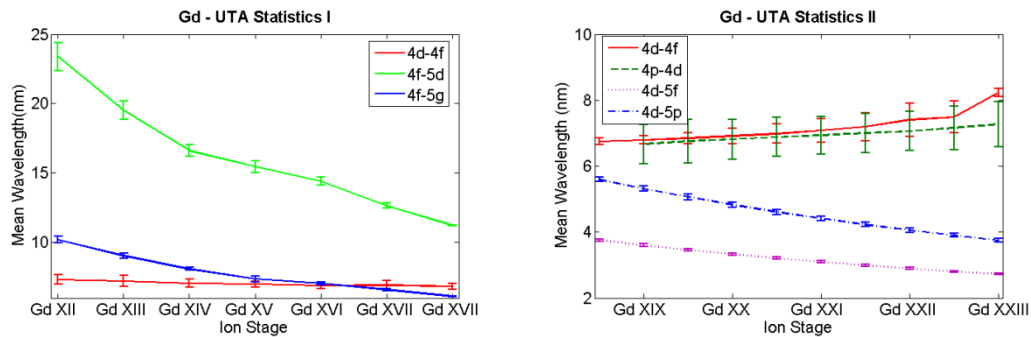


*Fig. 2: Calculated spectra (oscillator strength vs  $\lambda$ ) for Gd ions in the 6-8 nm spectral region.*

Plasma modeling calculations were performed using the collisional-radiative (CR) approach [15] which yielded the variation of ionic population as a function of electron temperature presented in Fig. 3. It is seen that the optimum plasma temperature needed to optimize the populations of Ag-like  $Gd^{17+}$ , Pd-like  $Gd^{18+}$  and Rh-like  $Gd^{19+}$  lies in the range 80-130 eV. The next step in the calculation was to calculate the emission at different ion temperatures by weighting the emission from each stage by the appropriate ion distribution after first populating the upper states with a Boltzmann distribution appropriate to that temperature. The resulting spectra are presented Fig. 4. It is clear from these simulated spectra that the optimum electron temperature is close to 110 eV, where the emission peak close to 6.76 nm is highest and the spectrum shows the highest spectral purity. This wavelength value is essentially the mean value for the most intense Ag- like emission. It should be noted that in this and subsequent figures, the theoretical spectra for  $Gd^{17+}$  and  $Gd^{18+}$  were shifted by approximately 0.06 nm and 0.02 nm respectively to longer wavelengths to bring them into close agreement with experimentally available data [17, 18] while the data for other ion stages were unshifted.

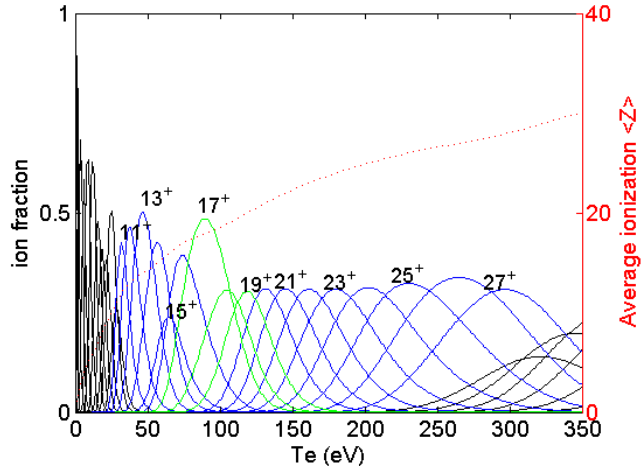


*Fig. 3: Mean wavelength and transition array width for the resonance transition in for different Gd ions. Left: ions with ground  $4d^{10}4f^n$  configurations; right: ions with  $4d^n$  ground configurations.*

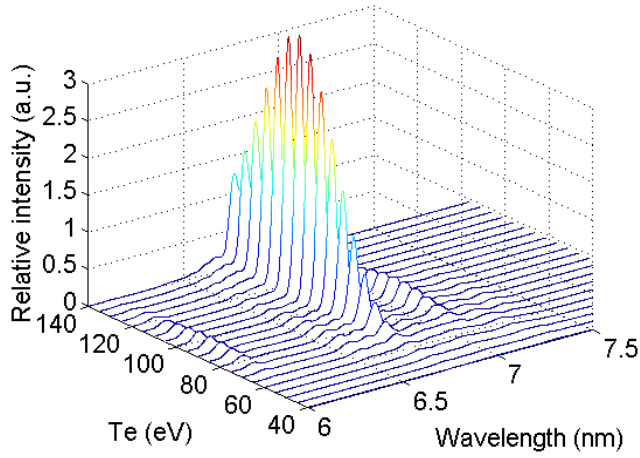


*Fig. 4: Theoretical Gd spectra as a function of electron temperature and wavelength.*

Comparisons between theoretical and experimental spectra are presented in Figs. 5 and 6. In Fig. 5 the theoretical spectrum is compared with the LPP data of [4] which gives a good fit for an electron temperature of 144 eV and



compares well with the earlier FAC code calculation which arrived at an identical value [5]. The laser flux on the target surface was estimated as  $(5 - 8) \times 10^{11} \text{ Wcm}^{-2}$  which yields an average electron temperature is around 135 – 180 eV [15]. While our value is above the calculated optimum value, the Ag and Pd like lines are clearly visible. While the present value is above the calculated optimum value, the Ag and Pd like lines are clearly visible. However while the agreement with the earlier calculation validates both approaches, the experimental spectrum is integrated over the full duration of a laser pulse and thus a range of plasma conditions. Moreover, the plasma from pure Gd is known to be optically thick since the emission profile is very sensitive to the Gd concentration in the target [7, 8, 19]. Self-absorption due to lower ionic charge states and neutral vapor in the expanding Gd plasmas will reduce the intensity at wavelengths greater than 6.8 nm. The resonant emission at 6.76 nm is therefore not absorbed by lower ion stages and is essentially unattenuated [20].

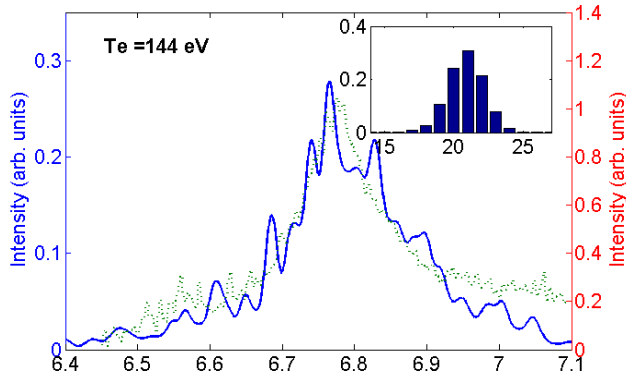


Fig. 5: Comparison between a laser produced plasma (LPP) experimental spectrum published in [4] (dotted line) and the numerical simulation (solid line). The relative populations of the contributing ion stages are presented in the inset.

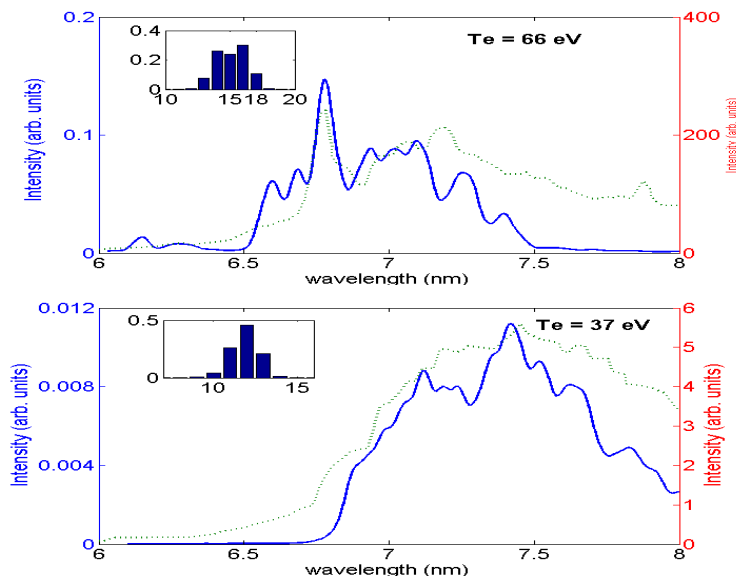


Fig. 6: Comparison between a discharge produced plasma (DPP) experimental spectra (dotted line) and the numerical simulation (solid line). The relative populations of the contributing ion stages are presented in the inset.

In Fig. 6 the theoretical spectra are compared to recent DPP results recorded with a microcapillary laser triggered discharge [21,22]. The electron density of the DPP is expected to be the order of  $10^{19}$ – $10^{20}$  cm<sup>-3</sup> again comparable to that in a Nd:YAG plasma. For a potassium discharge plasma produced in the same setup, at the same electron density, the optical depth for resonance 3p-3d transitions was evaluated as 5 μm so for the 4d-4f and 4p-4d transitions occurring in the 6-8 nm spectral region in Gd we anticipate a similar value [23, 24]. The Gd vapor was injected by laser ablation and was supplied along the discharge axis. A pair of electrodes was set around this axis inside the vacuum chamber. The discharge between the electrodes, produced with a pulsed power supply with a condenser capacity of 900 nF, was initiated by a laser triggered spark. The maximum discharge voltage and current, which were measured by a high voltage probe and a Rogowski coil, were 15 kV and 9 kA, respectively. The period and the discharge time of the discharge current were  $T = 3.5$  μs and 10 μs. The time-integrated spectra were measured by a thermoelectrically cooled back-illuminated x-ray charge coupled device (CCD) camera. The typical spectral resolution was better than 0.02 nm.

The delay time between the laser-trigger to start the discharge and the laser-ablation of Gd vapor could be changed. Fig. 6(a) was recorded at a

delay time of 1.1  $\mu\text{s}$  at a higher discharge current than 6(b) where the delay time was 6  $\mu\text{s}$ . The different initial Gd vapor density in the electrode gap, results in different plasma impedance and energy coupling. The emission intensity was observed to be maximized at the optimum delay time of 1.1  $\mu\text{s}$  in Fig. 6(a). In practice, since the experimental spectra are time integrated over a range of plasma conditions this agreement is somewhat fortuitous though it is indicative of the average temperature over that part of the plasma lifetime where spectral emission in the EUV is greatest. The spectra in Fig. 6 are best described in the model by electron temperatures of 66 and 37 eV respectively, which accounts for their low intensity, as the dominant ions at this temperature emit a broad weak array in the 7 – 8 nm region. In Figs. 5 and 6, the theoretical spectra are convolved with a Gaussian profile where the widths correspond to experimental resolutions of 0.007 nm and 0.02 nm, respectively.

In summary, the EUV emission spectra of Gd were calculated using the HFCl method. Even though no attempt was made to allow for opacity effects, synthetic spectra deduced from calculations within the CR framework compare very well with data from LPP and DPP experiments and suggest that the optimum electron temperature is close to 110 eV which gives maximum brightness at 6.76 nm. However the precise wavelength remains to be verified experimentally. Based on the results of [15] this electron temperature implies a laser flux close to  $2.4 \times 10^{11} \text{ W/cm}^2$  for a  $\text{CO}_2$  LPP. From initial experimental

studies [7,8] it is clear that LPPs produced by Nd:YAG lasers are optically thick. Further work is needed to find both the optimum temperature and source conditions using calculations that allow for full radiation transport and plasma hydrodynamics.

We would like to acknowledge support from Science Foundation Ireland under Principal Investigator grant no. 07/IN.1/I1771.

### **References:**

- [1] C. Wagner and N. Harned, *Nat. Photonics* **4**, 24 (2010).
- [2] V. Y. Banine, K. N. Koshelev and G. H. P. M. Swinckels, *J. Phys. D* **44**, 253001 (2011).
- [3] G. Tallents, E. Wagenaars, and G. Pert, *Nat. Photonics* **4**, 809 (2010).
- [4] S. S. Churilov, R. R. Kildiyarova, A. N. Ryabtsev, and S. V. Sadovsky, *Phys. Scr.* **80**, 045303 (2009).
- [5] D. Kilbane and G. O'Sullivan, *J. Appl. Phys.*, **108**, 104905 (2010)
- [6] A. Sasaki, K. Nishihara, A. Sunahara, H. Furukawa, T. Nishikawa, and F. Koike, *Appl. Phys. Lett.* **97**, 231501 (2010).
- [7] T. Otsuka, D. Kilbane, J. White, T. Higashiguchi, N. Yugami, T. Yatagai, W. Jiang, A. Endo, P. Dunne, and G. O'Sullivan, *Appl. Phys. Lett.* **97**, 111503 (2010).
- [8] T. Otsuka, D. Kilbane, T. Higashiguchi, N. Yugami, T. Yatagai, W. Jiang, A. Endo, P. Dunne, and G. O'Sullivan, *Appl. Phys. Lett.* **97**, 231503 (2010).

- [9] Fraunhofer IOF Annual Report, 2007 (Unpublished).
- [10] Y. Platonov, J. Rodriguez, M. Kries, E. Louis, T. Feigl and S. Yulin, Proc. 2011 International Workshop on EUV Lithography, Maui, Hawaii.
- [11] G. O'Sullivan and P.K. Carroll, *J. Opt. Soc. Am.*, **71**, 227 (1981)
- [12] R. D. Cowan, *The Theory of Atomic Structure and Spectra* (University of California Press, Berkeley, CA, 1981).
- [13] C. Bauche-Arnoult, J. Bauche, and M. Klapisch, *J. Opt. Soc. Am.* **68**, 1136 (1978)
- [14] G. O'Sullivan and B. W. Li, *Journal of Micro/Nanolithography, MEMS, and MOEMS*, (submitted).
- [15] D. G. Colombant and D. F. Tonon, *J. Appl. Phys.* **44**, 3524 (1973).
- [16] C. S. Harte, C. Suzuki, T. Kato, H. A. Sakaue, D. Kato, K. Sato, N. Tamura, S. Sudo, R. D'Arcy, E. Sokell, J. White and G. O'Sullivan, *J. Phys. B: At. Mol. Opt. Phys.* **43**, 205004 (2010).
- [17] J. Sugar, V. Kaufman and W. L. Rowan, *J. Opt. Soc. Am. B* **10**, 1321 (1993).
- [18] J. Sugar, V. Kaufman and W. L. Rowan, *J. Opt. Soc. Am. B* **10**, 799 (1993).
- [19] G. O'Sullivan and P. K. Carroll *J. Opt. Soc. Am.* **71**, 277 (1981).
- [20] T. Higashiguchi, T. Otsuka, N. Yugami, W. Jiang, A. Endo, B. Li, D. Kilbane, P. Dunne, and G. O'Sullivan, *Appl. Phys. Lett.* (accepted for publication, 2011).

- [21] T. Otsuka, B. W. Li, C. O’Gorman, T. Cummins, D. Kilbane, T. Higashiguchi, N. Yugami, W. H. Jiang, A. Endo, P. Dunne and G. O’Sullivan *Journal of Micro/Nanolithography, MEMS, and MOEMS*, (submitted).
- [22] T. Hosokai, T. Yokoyama, A. Zhidkov, H. Sato, K. Horioka, and E. Hotta, *J. Appl. Phys.* **104**, 053305 (2008).
- [23] T. Higashiguchi, H. Terauchi, T. Otsuka, M. Yamaguchi, K. Kikuchi, N. Yugami, T. Yatagai, W. Sasaki, R. D’Arcy, P. Dunne, and G. O’Sullivan, *J. Appl. Phys.* **109**, 013301 (2011).
- [24] T. Higashiguchi, M. Yamaguchi, T. Otsuka, H. Terauchi, N. Yugami, T. Yatagai, R. D’Arcy, P. Dunne, and G. O’Sullivan, *Appl. Phys. Lett.* **98**, 091503 (2011).